Available online at website: https://journal.bcrec.id/index.php/bcrec

Bulletin of Chemical Reaction Engineering & Catalysis, 20 (2) 2025, 280-292

Original Research Article

Silica Synthesis from Mount Semeru Volcanic Ash as a Nickel Heavy Metal Adsorbent

Raden Darmawan*, Sri Rachmania Juliastuti, Bagas Hardiatmoko, Aulia Defriana, Orchidea Rachmaniah, Fitria Nur Laily

Department of Chemical Engineering, Institut Teknologi Sepuluh Nopember, Jl Raya ITS, 60111, Surabaya, Indonesia

Received: 6th January 2025; Revised: 26th March 2025; Accepted: 29th March 2025
Available online: 3th April 2025; Published regularly: August 2025

Abstract

This study aims to synthesize SiO_2 gel-based adsorbents using the sol-gel method from Mount Semeru volcanic ash through varying concentrations of sodium hydroxide and acid catalysts and to determine its adsorption capacity on nickel (Ni(II)). Volcanic ash was obtained from Lumajang District, East Java, Indonesia. The silica gel adsorbent was made using the sol-gel method with different amounts of NaOH (1.0 M, 2.0 M, 3.0 M, and 4.0 M) and acid catalysts (acetic and hydrochloric acid). First, silica (SiO_2) was extracted from the volcanic ash, and then the sol-gel process was used to manufacture SiO2 gel-based adsorbents. The SiO_2 gel was analyzed using X-ray Fluorescence Analysis, Fourier-transform Infrared (FTIR), and Brunauer Emmett, and Teller (BET). Adsorption analysis of the Ni(II) metal ion content was conducted at various stirring rates and adsorbent dose masses. The results obtained showed that the most optimal SiO_2 gel was achieved when using 3.0 M NaOH, 10.53% HCl, and 8.30% CH_3COOH. Through FTIR analysis, NaOH 3.0 M x HCl silica contains only the siloxane groups, whereas NaOH 3.0 M x CH_3COOH silica contains both the silanol and siloxane groups. The best results were gained with SiO_2-based adsorbents (NaOH 3.0 M x CH_3COOH) at a dose of 10 g/L and a stirring rate of 50 rpm, with Ni(II) adsorption effectiveness of 99.80%.

Keywords: adsorbent; characterization; Mount Semeru; silica; sol-gel; volcanic ash

How to Cite: Darmawan, R., Juliastuti, S. R., Hardiatmoko, B., Defriana, A., Laily, F. N. (2025). Synthesis of Silica from Mount Semeru Volcanic Ash as an Adsorbent for Nickel Heavy Metal. *Bulletin of Chemical Reaction Engineering & Catalysis*, 20 (2), 280-292. (doi: 10.9767/bcrec.20337)

Permalink/DOI: https://doi.org/10.9767/bcrec.20337

1. Introduction

Mount Semeru is one of the most active volcanoes on the densely populated island of Java. This is because the mountain is directly adjacent to Lumajang and Malang Districts, of the province of East Java, Indonesia. Located at a longitude of 8.1° S, 112.9° E with a peak reaching 3,676 m above sea level [1,2]. As the most active volcano on the island of Java, it has erupted several times [3]. Monitoring records confirm that volcanic activity occurred in 1990, 1992, 1994, 2002, 2004, 2005, 2007, 2008 (2 times), 2020, and December 4th, 2021 [4]. Even though exactly 1 year has passed, Mount Semeru erupted on December 4th, 2022 at 2 a.m. Magma and gas from within the earth came out to the surface in the form of eruptions that expelled loose materials of various sizes, a mixture of these producing volcanic ash [5,6]. Volcanic ash consists of jagged pieces of rock, minerals, and volcanic glass that are hard, abrasive, and insoluble in water [7].

Volcanic ash as waste from the eruption process, must be utilized optimally. To support environmentally sustainable development

* Corresponding Author.
Email: rdarmawan@chem-eng.its.ac.id (R. Darmawan)

programs [8]. At first, the use of volcanic ash was only limited to cement-making [9]. Later on, has also been tested as an adsorbent for water purification processes from mixtures of dyes, anions, and metals [10]. A previous study reported the ability of coal fly ash to produce ZSM-zeolite [11]. The main material used coal fly ash was produced more pollutant in operation, so required process less than pollutant. Titchou *et al.* also reported that local Moroccan volcanic ash was used to adsorb cationic dyes (methylene blue), with a maximum absorption capacity of 43.86 mg/L [12]. On the other hand, Natale *et al.* also reported that volcanic ash can effectively eliminate mercury compared with those that are commercially available, such as activated carbon [13]. Therefore, based on these studies, volcanic ash has the potential to be developed as an adsorbent for chemical pollutants [14].

In the previous research, it showed that the synthesized silica (SiO_2) from geothermal solid waste using volcanic ashcontains high amounts of silica oxideand achieve adsorption effectiveness of 88.29% [15]. In this study, the volcanic ash was used as the source to synthesis silica. The volcanic ash was selected because it has a potential to be an adsorbent with a very high SiO_2 content (45 – 75%) [16–18]. This is also based on the presence of pores, silanol groups (-Si-O-H) and siloxane active sites (Si – O – Si) on its surface. The presence of four oxygen atoms in SiO_2, has quite ionic properties which serves as an active site for binding heavy metals, forming Si – Metal bonds. Besides that, Si can be used with Ag/HZSM-5 as the catalyst to support many chemical reaction processes [19]. This research aims to investigate raw minerals from the volcanic ash of Mount Semeru, especially Si. Nickel (Ni(II)) is a byproduct of the electroplating process and battery waste which has the potential to contaminate water. Its toxicity in water makes it a threat to the environment because it tends to bioaccumulate as it moves up the food [20]. Furthermore, Ni(II) is a carcinogen that can also result in skin irritation, kidney and lung issues, lung fibrosis, and digestive abnormalities [21].

Many research have focused on the techniques for removing these metals, including reverse osmosis, reduction, chemical oxidation, ultrafiltration, chemical precipitation, ion exchange, and electrolysis [22]. However, these technique still have inherent limitations including low efficiency, low sensitivity under operating conditions, large amounts of sludge in the generation process, and expensive disposal process costs [23]. However, adsorption is an effective technique in the removal of metal wastes. This is because metal wastes can be absorbed in large quantities, and have flexibility in terms of design so that adsorbents are cheap and can be regenerated [14,22].

Therefore, it is necessary to apply an adsorption process to eliminate Ni(II) by presenting an effective and sustainable adsorbent. One of them is by utilizing SiO_2 in volcanic ash. Although natural adsorbents, such as volcanic ash, have functional groups capable of absorbing pollutants in the aqueous phase, boosting the activation of basic or acidic chemicals can significantly increase the number of functional groups involved. To surface activate adsorbents, alkali metal hydroxides, such as potassium hydroxide (KOH) and sodium hydroxide (NaOH), are widely used [24]. In the case of the initial gel, the KOH is a network modifier which breaks the bonds between the condensed silicon species generating non-bridging oxygen atoms in sol gel process, the appearance of non bridging oxygens, resulting in charge defects in the structure. The ageing behavior with sodium hydroxide (NaOH) which stabilizing the initial silicate gel over the time, NaOH suggest the formation of higher order silicate species and therefore the polymerization of the structure [25]. However, the use of alkaline activators faces challenges due to the higher concentration requirements needed, only being able to operate at high conditions, and excessive treatment processes [26]. One method in anticipating this challenge is by utilizing acid as a surface stabilizer of the adsorbent and lowering the operating conditions of the process [27]. In this method, inorganic oxides with properties that include hardness, thermal resistance, optical transparency, and porosity, can be carried out at low temperatures [28].

Currently, the use of the sol-gel method in producing adsorbents is still limited [28]. Even the use of SiO_2-based adsorbents from volcanic ash is still limited to dye waste [1,10,26]. Although its use has been reported, the application of the sol-gel method is still limited to the use of strong acids such as hydrochloric acid (HCl) and sulfuric acid (H_2SO_4) [29–31]. There have been no reports of the synthesis of SiO_2-based adsorbents from volcanic ash using the sol–gel method with variations of strong and weak acids. The purpose of this study is to use the sol-gel method to synthesize and analyze SiO2 from Mount Semeru's volcanic ash. By altering the stirring speeds during the contact process, a study was also conducted to ascertain the SiO2 gel's adsorption capability from Mount Semeru volcanic ash on Ni(II). It is also expected that this study be able to present the techniques to obtain natural SiO_2-based adsorbents and increase their effectiveness and higher selectivity in the adsorption process of heavy metals in Ni(II)-containing wastewater which higher concentration than quality standard.

2. Materials and Methods

2.1 Materials

Volcanic ash from Mount Semeru was collected on March 14th, 2022 directly from Sumberurip Village, Pronojiwo Subdistrict, Lumajang District, East Java, Indonesia. The following were used: solid sodium hydroxide (NaOH) (37% hydrochloric acid solution) and 100% acetic acid solution -from Merck; nickel sulfate ($NiSO_4$) granule (Sigma-Aldrich); liquid waste (X industry (partner industry)) pH paper; filter paper, and distilled water (Merck). In the adsorption analysis of Ni(II), the following reagents were used: 98% ammonium persulfate (Sigma-Aldrich); 25% ammonium hydroxide (Merck); and dimethylglyoxime (Merck Milipore).

2.2 Experimental Device

In the adsorbent manufacturing process, the experimental device used includes a 200-micron sieve, 1000 mL beaker glasses (Iwaki Pyrex), porcelain cups, furnaces, hot plates, magnetic stirrers; and analytical balance (OHAUS).

2.3 Experimental Parameters and Conditions

The operating conditions in this study included 200-μ volcanic ash with a mass of 100 g. The calcination temperature was set at 750 °C for 4 h. Neutralization was done using a concentrated 1.0 M HCl solution with 250 mL per 100 g of calcined ash. The drying temperature was set at 110°C. The input variables were 1.0 M, 2.0 M, 3.0 M, 4.0 M NaOH, and the catalyst used 1.0 M HCl and 1.0 M acetic acid (CH_3COOH). Meanwhile, the adsorption analysis for Ni(II) was carried out using a 350-ppm $NiSO_4$. SiO_2 content of SiO_2 functional groups, SiO_2 area, and Ni(II) content in the solution following adsorptive treatment are the anticipated responses based on the established parameters.

2.4 Experimental Procedure

2.4.1 Extraction and analysis of SiO_2 elements from Mount Semeru Volcanic Ash

Calcination is the initial purification step used to eliminate surplus contaminants. Several metals are still present in volcanic ash after calcination. The amount of SiO_2 produced by volcanic ash is reduced when metals are present. In order to continue the soaking procedure with HCl, metal impurities must be removed by calcination. Semeru Mount volcanic ash was sifted using a 200-μ sieve. After obtaining 100 grams of volcanic ash as a result of sifting, that was placed in a porcelain cup and then calcined using a furnace at 750 °C for 4 h. The fine ash resulting from the calcination was washed using 250 mL of 1 M HCl solution through stirring for 1 h and left to stand for 24 hours, which was then tested for its acidity using universal pH paper. Then the ash was filtered using the filter paper and rinsed with distilled water until neutral. After that, it was tested again using universal pH paper. The fine volcanic ash was then dried in an oven at a temperature of 110 °C for 2 h. The dry ash was weighed and 1 g was taken to be analyzed using X-ray Fluoroscence Analysis. Furthermore, volcanic ash was used for the process of producing sodium silicate (Na_2SiO_3).

2.4.2 Preparation of the Na_2SiO_3 solution (Sol Method)

A total of 100 g of calcinated volcanic ash was mixed with 1,000 mL of NaOH according to the variable while stirring until boiling for 1 h. The mixture was allowed to cool, then the solution was filtered using filter paper and the brownish filtrate or Na_2SiO_3 precursor was used for the synthesis of SiO_2 gel.

2.4.3 Synthesis of SiO_2 gel (Gel method)

As much as 1,000 mL of the Na_2SiO_3 solution was placed in a container, after which, the catalyst (CH_3COOH and HCl) were added slowly according to the variable while stirring until a gel or Na_2SiO_3 solution was condensed with an acid solution to reach pH of 7. Then, the gel formed was allowed to stand for 24 h and filtered using filter paper. SiO_2 gel was dried in an oven at 110 °C for 1 h. Silica gel was then crushed and sieved. The synthesized SiO_2 gel was analyzed using the Fourier-transform Infrared Spectroscopy (FTIR) to determine the functional groups and other characterization methods.

2.5 Characterization Procedure

2.5.1 X-Ray Fluorescence (XRF) Method

This analysis was used to analyze the chemical elements and the amount contained in the volcanic ash of Mount Semeru. XRF uses X-ray radiation. Specifications for the XRF tool with the PANanalytical brand, minipal type 4. The method used is without standards and filters. Air medium, with 30 KV energy. The temperature read is 22.9 °C and the humidity is 66%.

2.5.2 X-Ray Diffraction (XRD) Method

This XRD examination was carried out at 800 °C and 1000 °C for 1 h. Using a Rigaku Miniflex II X-ray diffractometer equipped with Cu-Kα (λ = 1.54056 angstroms), the resultant SiO2 was analyzed. XRD patterns were gathered using a 2θ range of 15 to 60° and a step size of 0.02°.

2.5.3 Fourier Transform Infra Red (FTIR) Method

With a spectrum range of 7,800–350 cm^{-1}, the Thermo Scientific FTIR, Nicolet IS10 was used. The purpose of FTIR was to determine whether chemicals have functional groups. Infrared spectrophotometry will be used to analyze the SiO_2 gel sample that was first created with a comparison of the synthesis concentration. The wavenumber data (cm-1) used in this test came from data that allowed the functional groups in the compound to be identified based on the functional group data range that was available.

2.5.4 Adsorption analysis of Ni(II) (SNI 6989.16:2009)

As much as 1000 mL of $NiSO_4$ solution according to the variable concentration (100 ppm and 350 ppm) was added to the synthesized SiO_2 gel at the doses according to the variable (5 g and 10 g). Stirring was carried out with a variable rate of 50 rpm, 100 rpm, and a mixture rate of 100 rpm for 1 h and then continued with 50 rpm. Every 30 min, samples of the solution were collected to test for Ni(II) content after placing it in contact with SiO_2 gel for 6 h. The Ni(II) content test was carried out through filtration of the collected sample. For every 3 mL of sample, 5 mL of ammonium persulfate was added. The sample was allowed to stand for 10 min, after which 3 mL of ammonium hydroxide and 3 mL of dimethylglyoxime were added. A total of 50 mL of distilled water was added and the solution was left to stand for 15 min. Furthermore, the Ni(II) content in the sample was read using a UV-Vis spectrophotometer with a wavelength of 450 nm. In the adsorption analysis for metal ion levels, the adsorption effectiveness of ion levels is also calculated using the Equation (1).

$$Adsorption\ effectivity = \frac{C_t - C_0}{C_0}\ x\ 100\% \qquad (1)$$

where, C_t denotes Ni^{2+} concentration at t-minute, and C_o expresses initial concentration.

2.5.5 Brunauer, Emmett and Teller (BET) Method

We used Quantachrome TouchWin version 1.2 with St 2 specifications on NOVA 4LX for BET analysis. This tool is used to analyze specific surface area and porosity using the principle of physical adsorption (physisorption). In physisorption, a certain amount of inert gas, at a very low temperature (77 ^oK), and vacuum pressure was adsorbed on the surface of the adsorbent. This physisorption does not depend on the nature of the adsorbent but only depends on the specific surface area and pore structure. The specific surface area of the analyzed adsorbent (sample) is measured by the number of molecules deposited (adsorbed) in the monolayer. Meanwhile, the pore size is determined by the condensation pressure (evaporation pressure) of the gas in the pores [32].

3. Results and Discussion

3.1. Characterization of Mount Semeru Volcanic Ash

Volcanic ash (<2 mm to the size of dust) comes from fragments/ or fallen volcanic material that is ejected into the air during an eruption [33]. Physically, the volcanic ash collected sample from Mount Semeru was very fine grayish powder. This volcanic ash was crushed and then sieved to homogenize the size of the ash particles and expand its surface so that the synthesis of Na_2SiO_3 is effective. Furthermore, the initial composition or content of the volcanic ash was analyzed using XRF.

Table 1 shows that the main components of Mount Semeru's volcanic ash include Al (8.35%), Si (27.25%), Ca (25.15%), and Fe (31.30%). Other components are in small amounts: Mg, P, S, K, Ti, V, Mn, Cu, Zn, Sr, Y, Zr, Ba, and Re. Data on the composition of the volcanic ash for Si in the form of oxide contains SiO_2. This shows that the Semeru volcanic ash taken is of the basal type because it has a SiO_2 content of <55%. This type of basalt originates from low-energy eruptions, producing dark, fine-grained igneous rocks that are generally frozen lava from volcanoes [33, 34].

The presence of metals in the volcanic ash causes the yield of SiO_2 to decrease. Therefore, it is necessary to free metal impurities using the calcination process and continue the soaking process. Soaking volcanic ash with strong acid, namely, HCl, is believed to enable the removal of the metals present in it [34]. Furthermore,

Table 1. Chemical composition of Mount Semeru volcanic ash

Element	Quantity (%)	Oxide Element	Quantity (%)
Al	8.35	Al_2O_3	11.50
Si	27.25	SiO_2	38.90
P	0.95	P_2O_5	1.00
S	0.06	SO_3	0.09
K	2.68	K_2O	1.95
Ca	25.15	CaO	20.45
Ti	1.70	TiO_2	1.55
V	0.06	V_2O_5	0.06
Mn	0.78	MnO	0.51
Fe	31.30	Fe_2O_3	22.70
Cu	0.32	CuO	0.19
Zn	0.06	ZnO	0.05
Sr	0.74	SrO	0.42
Y	0.04	Y_2O_3	0.04
Zr	0.12	ZrO_2	0.073
Ba	0.35	BaO	0.20
Re	0.09	Re_2O_7	0.03

Worathanakul *et al.* also reported that the acid soaking method increased the SiO_2 composition in the ash and the SiO_2 composition obtained was slightly higher, at 89% [37]. The use of HCl in the purification process is due to the chemical nature of SiO_2 which is insoluble/ or reactive toward acids except for HF, so it does not reduce the yield of the SiO_2 formed. HCl is a strong acid that dissociates completely in water to become H^+ and Cl^-. Metal impurities in the form of metal oxides are bases that when reacted with water form an alkaline solution (pH> 7). This alkaline mixed solution still contains a lot of impurities. So if the metal oxide is reacted with HCl, there will be a reaction between the metal oxide in the form of a base and the acidic solution of HCl to form salts and water molecules. Meanwhile, $SiO_{2(s)}$ contained in the sample cannot be dissolved with HCl because SiO_2 is an acidic oxide that will react with alkaline solutions; thus, $SiO_{2(s)}$ is still present in the residue [38].

The salt produced in this washing process has great solubility in water so the metal oxide which is an impurity in the form of a chloride salt will dissolve. To maximize the washing process, continuous stirring was carried out for 1 h. Furthermore, filtration, which aims to separate the residue ($SiO_{2(s)}$) from the impurity solution was applied. This residue is used as a precursor for the next process. The reduced metal impurities are expected to increase the SiO_2 purity. The composition of Mount Semeru volcanic ash that has been calcined and soaked with strong acid using HCl is shown in Table 2.

3.2. Production of Silica-Based Adsorbents from Mount Semeru Volcanic Ash

After calcination and immersion, the volcanic ash was then melted with NaOH according to the variables (1.0 M, 2.0 M, 3.0 M, and 4.0 M) using the sol method to form Na_2SiO_3. Melting at high temperatures causes NaOH to melt and completely dissociate to form Na^+ and OH^- ions. The high electronegativity of the O atom in SiO_2 causes Si to be more electropositive and the unstable intermediate $[SiO_2OH]^-$ is formed which is unstable and dehydrogenation . The second OH^- ion can make a bond with hydrogen become a water molecule and two Na^+ ions. It balances the negative charge of the SiO_3^{2-} ion to form Na_2SiO_3 [17,39,40]. The initial indicator for the formation of sodium silicate is that when touched the solution feels slippery on the skin. Solid SiO_2 and oxides are not decomposed.

The formed Na_2SiO_3 is then added to the acid solution according to the variable. The addition of acid to Na_2SiO_3 sodium silicate solution results in the exchange of Na^+ and H^+ ions to form free silicic acid (H_2SiO_3), which is insoluble in acid. The H_2SiO_3 formed undergoes polycondensation reactions to form dimers, trimers, and so on while releasing water molecules. The reaction continues until a product in the form of SiO_2 gel is formed [41]. The SiO_2 gel obtained was allowed to stand for a day until a dry gel (xerogel) was formed and then weighed. The mechanism for the formation of Na_2SiO_3 is described by Figure 1.

Table 3 shows that the greater the concentration of NaOH used, the greater the mass of the SiO_2 adsorbent produced on various catalysts. The largest mass of the adsorbent was obtained when a catalyst concentration of 3.0 M . These results are consistent with those of Kalapathy *et al.* who found that SiO_2 increases at pH > 1050). Due to the low NaOH concentration (1.0 M and 2.0 M), the amount of SiO_2 from the ash which is bound to Na_2SiO_3 is relatively small. Meanwhile, at a concentration of 4,0 M NaOH, the weight of the resulting SiO_2 gel decreased compared with that of a concentration of 3.0 M. This was because the higher the concentration, the viscosity of the NaOH solution also increased,

Table 2. Chemical composition of Mount Semeru volcanic ash after calcination.

Element	Quantity (%)	Oxide Element	Quantity (%)
Al	8.30	Al_2O_3	11.00
Si	31.6	SiO_2	44.60
K	2.82	K_2O	2.00
Ca	24.00	CaO	19.10
Ti	1.80	TiO_2	1.59
V	0.05	V_2O_5	0.05
Mn	0.73	MnO	0.47
Fe	29.00	Fe_2O_3	20.40
Cu	0.25	CuO	0.14
Zn	0.06	ZnO	0.03
Sr	0.60	SrO	0.33
Zr	0,09	ZrO_2	0.06
Ba	0.40	BaO	0.20
Re	0.07	Re_2O_7	0.04

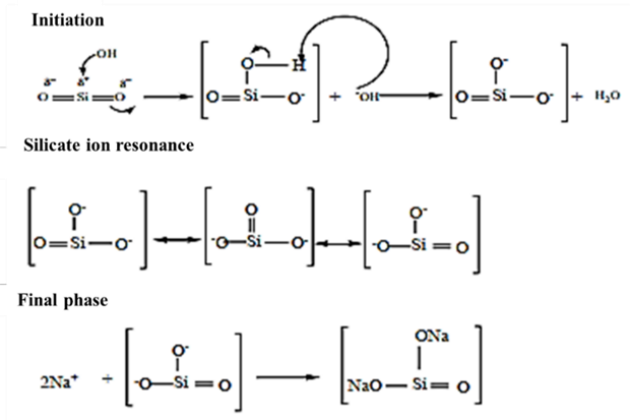

Figure 1. The reaction mechanism for the formation of sodium silicate.

thereby reducing the activity of ions in the solution. The lack of activity of these ions resulted in a decrease in the number of bonds formed between NaOH and SiO_2 in the volcanic ash [42].

Table 3 also shows that the formation of SiO_2 gel with the strong acid HCl catalyst produces a larger mass of SiO_2 than the weak acid catalyst CH_3COOH. This is related to the rate of formation of SiO_2 gel. In addition, this is because using HCl in the SiO_2 extraction process produces NaCl salt, thus the solution is neutral. In contrast, using CH_3COOH in the SiO_2 extraction process produces CH_3COON salt, thus the solution is alkaline. Based on the literature, SiO_2 dissolves easily under alkaline conditions but will form precipitates under neutral or acidic conditions. The alkaline nature of the solution causes a slower process of forming or precipitating SiO_2 gel to be slower because SiO_2 tends to dissolve rather than precipitate [43]. Furthermore, the xerogel was crushed to widen the specific surface area of the SiO_2 gel so that metal absorption would be more optimal when applied as an adsorbent.

3.3. Characterization of SiO_2 Gel Based on FTIR Method

FTIR is used to identify the molecular functional groups present in the synthesized SiO_2. The results of the FTIR test are presented in a graph showing the wavelengths on the x-axis and the amount of reflected light or the percentage (%) transmittance on the y-axis, as shown in Figure 2. Figure 2 shows the presence of an absorption band at wave number 434.83 cm^{-1}, namely silanol (Si–O). The strong absorption band is seen at wave number 1000.36 cm^{-1} which is the Si-O asymmetric strain of siloxane (Si–O–Si). At wave number 1,637.50 cm^{-1}, there is an -OH bend of the water molecule. At wave number 3,390.54 cm^{-1}, absorption appears which represents the -OH strain from the (Si–OH) group. Figure 2b. shows the presence of an absorption band at wave number 468.49 cm^{-1}, namely the vibration of the Si- group O functional group. At wave number 638.12 cm^{-1}, there is an asymmetric Si- group O strain. The strain symmetry of Si- group O on polysiloxane (Si–O–Si) is found at wave number 795.39 cm^{-1}. The wave number of 1,017.12 cm^{-1} is a very strong asymmetrical strain of siloxane (Si–O–Si). The -OH bend of (Si–OH) is found at wave numbers 1,636.74 cm^{-1} and 1,686.68 cm^{-1}. At wave numbers, 3,200-3,410 cm^{-1} absorption appears indicating strong Si–OH bonds from silanol (Si-OH) (hydrogen-bonded OH) [46]. At wave number 1,407.96 cm^{-1}, there is an absorption band indicating the presence of the Si–$CH{=}CH_2$ bend. In addition, the absorption wavelength of 1,017.12 cm^{-1} is a very strong asymmetric strain of siloxane (Si–O–Si). The band that supports the existence of the Si-O bond appears at wave number 638.12 cm^{-1}. Wave number 3,408.46 cm^{-1} indicates the vibration range of the -OH group from silanol (Si-OH), the presence of OH groups is emphasized by the presence of infrared spectral peaks at wave numbers 1,636.74 cm^{-1} and 1,686.68 cm^{-1} indicating the presence of bend in the –OH group of Si–OH. The wave number is 1,017.12 cm^{-1} which indicates the Si–O strain vibration of Si–O–Si. The band that supports the existence of the Si–O bond appears at wave number 638.12 cm^{-1} [17, 45].

The results obtained were compared with the SiO_2 gel Kiesel Gel 60 G made by E'Merck which is one of the commercial SiO_2 gels that has been circulating and is widely used as an adsorbent. The FTIR spectrum of Kiesel Gel 60 G showed the presence of Si–O–Si bent groups at the absorption band of 471.50 cm^{-1}. At a wavelength of 602.31 cm^{-1}, there is an asymmetric Si–O–Si strain group. The Si–O asymmetric strain function group is found in the absorption band at a wavelength of 1,111.12 cm^{-1}. At a wavelength of 1,636.03 cm^{-1},

Table 3. Mass synthesis of silica adsorbent from volcanic ash at various concentrations of NaOH and catalyst.

Catalyst	NaOH concentration (N)	The weight of the silica gel (g)
HCl	1.0	2.25
	2.0	4.12
	3.0	10.53
	4.0	2.14
CH_3COOH	1.0	1.77
	2.0	3.94
	3.0	8.30
	4.0	3.63

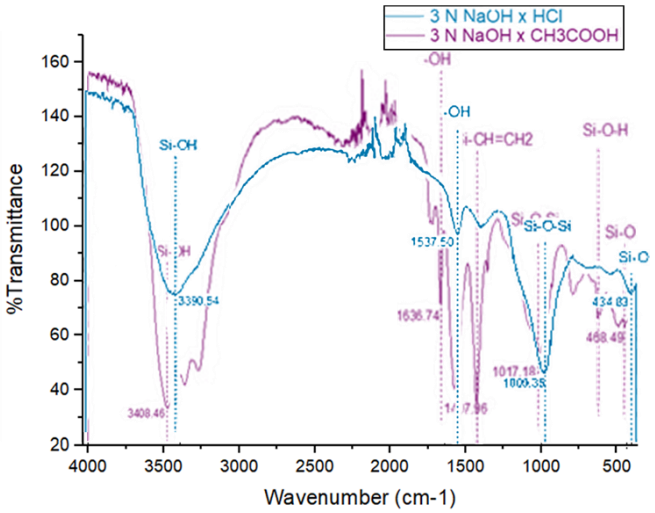

Figure 2. FTIR spectra of silica gel when NaOH 3.0 M and HCl and CH_3COOH catalysts.

there is a -OH bend. The Si–OH strain group is present in the absorption band with a wavelength of 3,459.34 cm^{-1} [46,47]. Based on this comparison, it can be concluded that the FTIR test gave a positive result, meaning that the SiO_2 gel from the research has a chemical structure, molecular formula, and functional groups. that are identical to that of the Kiesel Gel 60 G, which is a commercial SiO_2 gel.

Figure 3a shows the specific surface area of SiO_2 (NaOH 3.0 M x HCl) of 621 m^2/g, while Figure 3b. shows the specific surface area of SiO_2 (NaOH 3.0 M x CH_3COOH) of 588 m^2/g. Increased surface area has a stronger influence on nickel ion adsorption. The adsorption process greatly benefits from the larger internal surface area that smaller particles frequently possess. Smaller particles provide metal ions a shorter diffusion channel, increasing surface area and creating more active sites for adsorption. This results in faster and more effective mass transfer [47].

If the data obtained is compared with SiO_2 gel 60 G E'Merck with a specific surface area of 480-540 m^2/g. The results obtained from this study were greater than the SiO_2 gel 60 G E'Merck. In addition, compared with the results of the SiO_2 gel from chitosan, the specific surface area data from the SiO_2 gel in this study also obtained greater results (359 m^2/g for the chitosan SiO_2 gel [48]. Compared with previous studies, the synthesis of silica gel from Tunisian sand has a specific surface area of only 340 m^2/g [49]. This is because volcanic ash has a very high SiO_2 content, so the calcination process, the pores expand, and the surface area becomes larger [16,17]. Therefore, the results showed that the SiO_2 gel of this study has a much wider specific surface area, making it suitable for use as an adsorbent.

Greater surface area has such greater adsorption effects on nickel ion. Smaller particles often have a bigger interior surface area, which is extremely beneficial to the adsorption process. Increased surface area creates more active sites for metal ions to adhere, smaller particles provide a shorter diffusion channel for metal ions, which accelerates mass transfer and provides more efficient and quicker adsorption.

3.4. Adsorption Power of Synthesized SiO_2 on Ni(II) Metal Ions

A review of the adsorption capacity of SiO_2 on Ni(II) metal ions was carried out by varying the mass of the adsorbent and the rate of stirring. Figure 4, shows the process that occurs in the binding of metal ions and Ni(II) involves the Si–OH and siloxane Si–O–Si groups which are ionic interactions that also experience covalent interactions. This supports the assumption of Pearson's rule that the interaction of Ni(II) with solids is a chemical interaction, namely an acid-base interaction. Chemical interactions occur due to the formation of bonds between the active sites, namely the Si–OH and Si–O–Si groups of the adsorbent and the adsorbed substance. The bond between the Ni(II) metal ion and the active group on SiO_2 gel through the formation of a coordination bond, the lone pair of O on Si–OH will occupy the empty orbital owned by the Ni(II) ion so that a coordination complex is formed. The following is the reaction for the binding of Ni(II) metal ions to the Si–OH and Si–O–Si groups [46]. Moreover, SiO_2 can be desorbed and can be used after adsorption, however the adsorption capacity reduced.

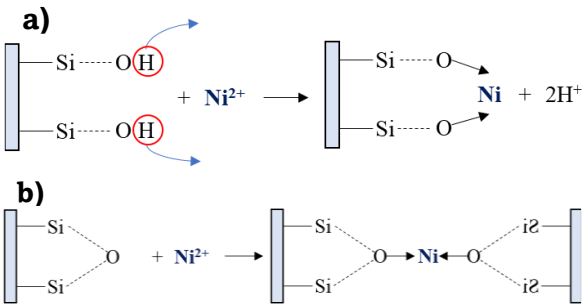

Figure 4. The reaction of the binding of Ni(II) metal ions to a). silanol group and b). siloxane groups.

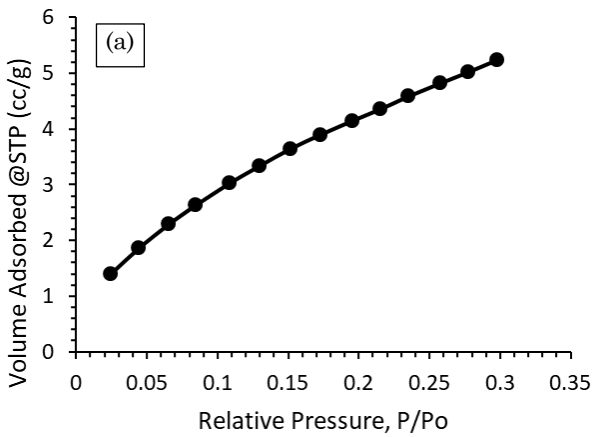

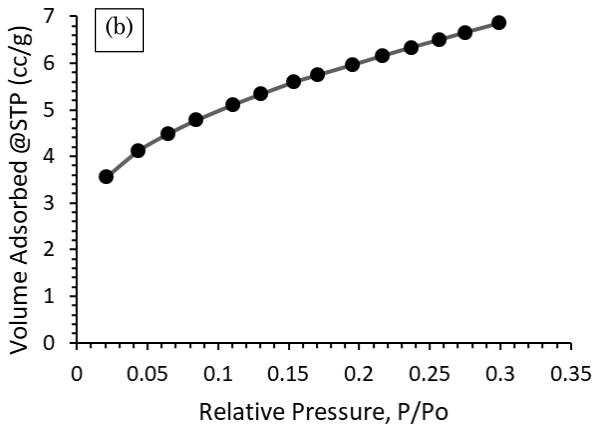

Figure 3. (a) Results of BET analysis of Silica Gel on NaOH 3.0 M x HCl and (b). Results of BET analysis of Silica Gel on NaOH 3.0 M x CH_3COOH.

The strength of the complex formation between metal ions and ligands depends, among other things, on the polarizing ability of these metal ions which is influenced by the ratio between the charge and the ionic radius. Small ions with a high charge have a greater bond strength than large which have a low charge [50]. Figure 5a. shows that the most optimal decrease in Ni(II) content occurs when stirring at 50 rpm by reaching a remaining Ni(II) content of 0.56 ppm at 300 min. Meanwhile, Figure 5b. shows a decrease in Ni(II) content when using SiO_2-based adsorbent (NaOH x CH_3COOH), which is the most optimal and also occurs when stirring at 50 rpm with a remaining Ni(II) content of 0.56 ppm at 240 min. This is because the use of a stirring rate that is too large results in the release of the bond between the adsorbent and the adsorbate, and the adsorbent structure is quickly damaged as a result of adsorption process that is not optimal [51]. Similar results were also reported by several researchers who showed a decreasing trend with increasing stirring rates [38,52].

A review regarding the mass variation of the adsorbent was carried out at an initial Ni(II) concentration of 350 ppm using adsorbent mass doses of 5 and 10 g/L. The results of the experiment of variations in giving adsorbent mass to the adsorption of Ni(II) metal ions using SiO_2 can be seen in the Figure 6. Figure 6, shows that there is a decrease in Ni(II) content for each use of the SiO_2 adsorbent at various mass doses. This shows that the use of each dose can reduce Ni(II) levels in the sense that it can absorb Ni(II) metal in a sample.

To review the effectiveness of the optimal dose, the adsorption effectiveness calculation is conducted. The adsorption effectiveness calculation data is shown in Table 4. Table 4 shows that the relationship between the mass of the adsorbent and the adsorption effectiveness percentage is directly proportional to the increase in the mass of the adsorbent. The higher the mass of the adsorbent used, the higher the effectiveness percentage of metal adsorption. This is because the concentration of metal ions decreases with an increasing amount of adsorbent used. Using the SiO_2 adsorbent for 300 min (3.0 M NaOH x HCl) at a dose of 5 g/L adsorbed 62.88% whereas a dose of 10 g/L adsorbed 90.48%. Meanwhile, (3.0 M NaOH x CH_3COOH) at a dose of 5 g/L SiO_2 adsorbed 71.40% and 99.80% at a dose of 10 g/L. The greater the amount of adsorbent, the greater the absorption of metal ions in a solution, thus the adsorption effectiveness percentage also increases [53]. Therefore, it can be said that the more adsorbent mass used, the greater the absorption efficiency of Ni(II) metal ions. The increase in the mass of SiO_2 gel is proportional to the increase in the number of particles in the adsorbent, causing an increase in the adsorption active site and an increase in absorption efficiency.SiO_2 gel contains Si–OH and Si–O–Si active group, thus the –O group on the two groups binds the Ni(II) metal ion. The bond between the metal ion and –O in Si–OH and Si–O–Si is through the formation of a

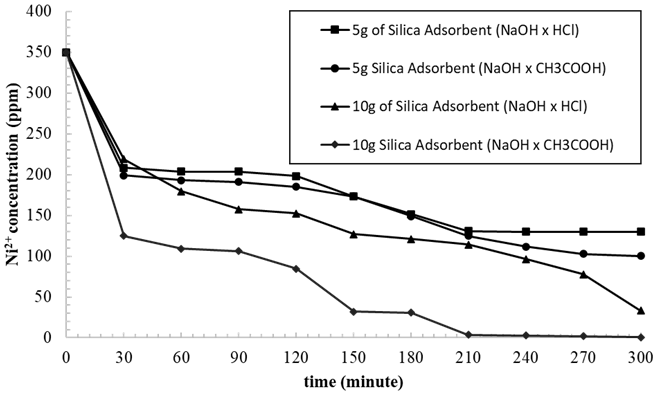

Figure 6. Decreased nickel levels using silica at doses of 5 g/L and 10 g/L.

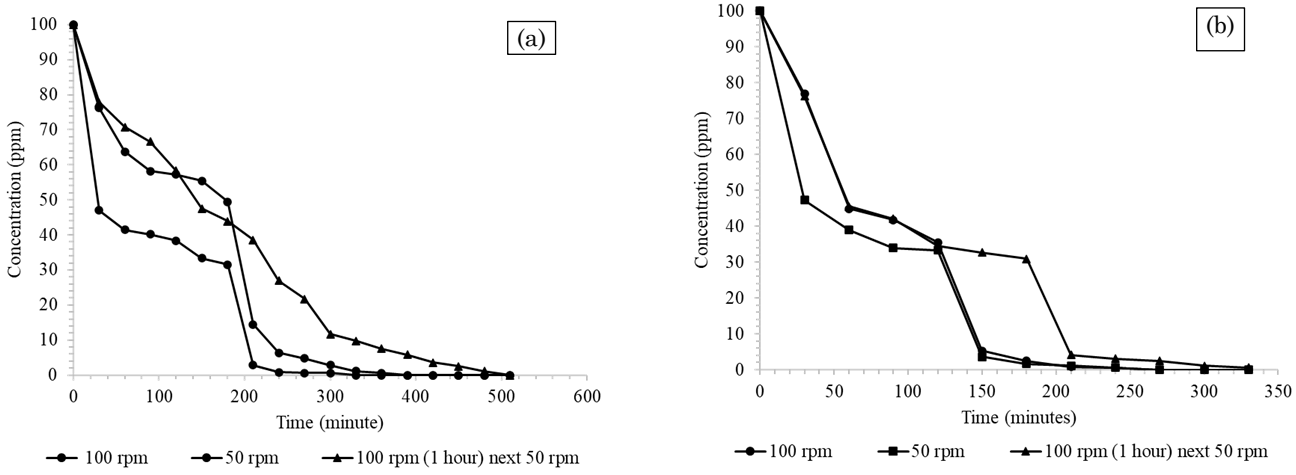

Figure 5. (a) Decreasing nickel content using silica-based adsorbents (NaOH x HCl) and (b). Decreasing nickel content using silica-based adsorbents (NaOH x CH_3COOH) through variations in stirring rate.

coordination bond, in which the lone pair of O on –OH will occupy the empty orbital owned by the metal ion to form a coordination complex. The interaction that occurs between the adsorbent and the adsorbate is a physical bond or physisorption. This weak bond is due to van der Waals forces, especially ion-dipole forces. This ion-dipole force is an electrostatic interaction that occurs between an ion (can be a cation or anion) with a polar molecule. This force is caused by Ni(II) attached to O- which is bound to Si-OH and Si-O-Si, where the hydrogen bonds between O and H are released due to electropositive competition between H^+ and Ni(II), forming Si–OH and Si–O–Si [38].

3.4.1 Adsorption of Ni(II) waste in industry X (partner industry)

The problem of high Ni(II) metal content in waste from partner industries is taken as a focus in wastewater treatment in this study. The initial concentration of Ni(II) waste is diluted to 300 ppm. The sample used was SiO_2 synthesized from 3.0 M NaOH x CH_3COOH. This is because the surface area of SiO_2 from 3.0 M NaOH x CH_3COOH is larger than that of SiO_2 formed from 3.0 M NaOH x HCl. Table 5 shows the waste quality standard as well as the comparison with the quality of the waste test results that have been carried out. It can be seen that the adsorption process can be carried out on industrial waste containing Ni(II) metal. Based on previous study, the adsorbent that is formed is also able to absorb other metals, such as Cu, Cr, Cd, and Pb, which based adsorbents can absorb heavy metals from industrial processes [23,53,54].

Table 4. Data on the effectiveness percentage of nickel adsorption at 300 minutes using silica adsorbent according to the mass dose of the adsorbent.

Silica Adsorbent	Dose (g/L)	Adsorption effectivity (%)
Silica adsorbent 3.0 M NaOH x HCl	5	62.88
	10	90.48
Silika adsorbent 3.0 M NaOH x CH_3COOH	5	71.40
	10	99.80

3.5 Characterization Based on X-ray diffraction (XRD)

The crystallinity of the samples was analyzed using XRD. The diffraction profiles the (NaOH x HCl) and (NaOH x CH_3COOH) samples were compared and shown in Figure 7. There were some differences terms of the position point. However there was same peak at 31.713° corresponding to used (NaOH x HCl) and (NaOH x CH_3COOH) samples. The same peak at 31.713° was also the maximum peak of all point in the diffraction profile, that was achieved 2,166.52. Peak at 31.73° was related to (NaOH x HCl) and (NaOH x CH_3COOH) because based on Figure 7 at position 31.73° both have peak. However (NaOH x CH_3COOH) has the optimum peak at 2,166.52. (NaOH x HCl) has the optimum peak at

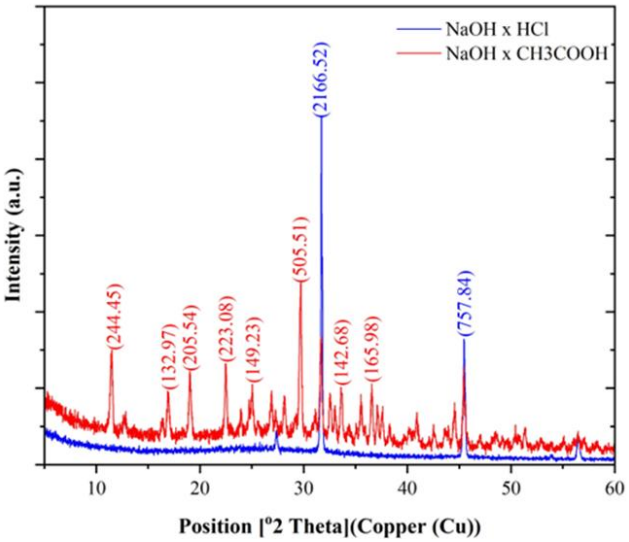

Figure 7. XRD analysis of Silica Gel on NaOH 3.0 M x HCl and on NaOH 3.0 M x CH_3COOH.

Table 5. Data on the comparison of the quality of waste content in industry X before and after the adsorption proces.

Parameter	Maximum Content from East Java Governor Regulation No. 72 in 2013 (mg/L)	Levels in effluent samples (mg/L)	Levels in sewage samples after treatment (mg/L)
TSS	20	5	5
Nickel (Ni)	1.0	3226	0.68
Chrome (Cr^{6+})	0.1	1.88	0.02
Copper (Cu)	0.6	36.1	0.15
Zinc (Zn)	1.0	21.8	1.98
Cadmium (Cd)	0.05	0.98	0.03
Lead (Pb)	0.1	3.15	0.16
pH	6.0 - 9.0	7.5	7.5

30° which achieved 505.51. The highest intensity point was showed the higher energies, which indicates the possible formation of multicomponent product [55]. When the peaks on XRD were open out it showed that the crystalline size was decreased from a bulk size to the nanoscale dimension [56]. Based on the review of Asif Ali, the arrangement of diffraction angles shows the arrangement of atoms. In crystalline materials, the results of XRD readings show clear peak differences due to the periodic arrangement of atoms, while amorphous materials show unclear peak differences [2]. As shown in Figure 7 the results of the crystalline materials are similar to the XRD results of (NaOH x HCl), while the XRD results of (NaOH x CH_3COOH) show an amorphous material.

Table 6 shows the composition of the examined samples determined based on XRD patterns. The analysis showed that Pd and Be were the dominant mineral compositions of the sample with the highest percentage in both (NaOH x HCl) and (NaOH x CH_3COOH) samples; however, besides that, it also consists of another composition. In the (NaOH x CH_3COOH) sample, some compounds are present: zirconium nickel antimonide (0.6265), terbium zinc antimonide (0.6009), strontium barium nitridotungstate (0.6182), silver(I) p-isocyanobenzoate (0.6629), rubidium magnesium leucite (0.6735), potassium zinc silicon oxide (0.6420), mercuric iodide (0.6202), manganese ditellurite (0.6205), and iron oxide (0.6134), among others. In contrast, the (NaOH x HCl) sample only has two other compounds: Nitrogen (0.6257) and Carbon (II) oxide (0.6088). The different sample compositions cause the resulting crystal shapes to be different. The sample with the highest material composition (NaOH x CH_3COOH) causes an amorphous form, while the sample with a low material composition (NaOH x HCl) causes a better crystalline form [57].

4. Conclusions

SiO_2-based adsorbent from Mount Semeru volcanic ash can be synthesized by the sol-gel method using NaOH with various acid solutions as a catalyst. The most optimal synthesis of SiO_2-based adsorbents from volcanic ash was obtained using 3.0 NaOH solution for each HCl (10.53%) and CH_3COOH (8.30%) catalysts, respectively, 10.53% and 8.30%. Through FTIR analysis of the two adsorbents obtained, in the (NaOH 3.0 M x HCl) SiO_2, there a Si–O–Si groups, whereas in the (NaOH 3.0 M x CH_3COOH) SiO_2, there are Si–OH and Si–O–Si groups. In addition, the optimal stirring rate for absorbing Ni(II) is 50 rpm and takes 240 min until the remaining Ni(II) content is 0.56 mg/L. Variations in the adsorbent mass (5 and 10 g/L) were also applied for each of the SiO_2 gels formed. Moreover, based on the XRD result, the crystal from (NaOH x HCl) produced better than that of (NaOH x CH_3COOH). The best results were obtained by using a SiO_2-based adsorbent (NaOH 3.0 M x CH_3COOH) at a dose of 10 g/L with a Ni(II) adsorption effectiveness percentage of 99.80%.

Table 6. Data on element composition of Silica Gel on NaOH 3.0 M x HCl and on NaOH 3.0 M x CH_3COOH.

Element	Percentage (%)
Pd	92.2
Be	7.8

Acknowledgement

The authors would like to thank the Directorate of Research and Community Service, Institut Teknologi Sepuluh Nopember, Indonesia (DRPM-ITS) for supporting and funding this project under Funding Work Department Batch 1 (Grant Number: 1008/PKS/ITS/2024).

CRediT Author Statement

Author Contributions: Raden Darmawan: Conceptualization, Investigation, Funding acquisition, Writing - review & editing, Supervision, Sri Rachmania Juliastuti: Conceptualization, Methodology, Orchidea Rachmaniah: Conceptualization, Bagas Hardiatmoko and Aulia Defriana: Data curation, Formal analysis, Investigation, Methodology, Fitria Nur Laily: Writing – review & editing. All authors have read and approved the final version of the manuscript.

References

[1] Aigbe, U.O., Ukhurebor, K.E., Onyancha, R.B., Osibote, O.A., Darmokoesoemo, H., Kusuma, H.S. (2021). Fly ash-based adsorbent for adsorption of heavy metals and dyes from aqueous solution: a review. *Journal of Materials Research and Technology*, 14, 2751-2774. DOI: 10.1016/j.jmrt.2021.07.140.

[2] Ali, A., Chiang, Y.W., Santos, R.M. (2022). X-ray diffraction techniques for mineral characterization: A review for engineers of the fundamentals, applications, and research directions. *Minerals*, 12(2), 205. DOI: 10.3390/min12020205

[3] Realita, A., Fahmi, M.N., Prastowo, T. (2022). Madlazim. Detection of Lahar Flow Direction from Semeru Eruption on 4 December 2021 using Gravity Method. *Journal of Physical Science and Engineering*, 7(2), 75-85. DOI: 10.17977/um024v7i22022p075.

[4] Wibowo, A. (2021). Estimating the Volcanic Ash Plume Course, PM2. 5 Emissions, and Environmental Impacts Based on the December 4, 2021, *Mount Semeru Eruption*. DOI: 10.20944/preprints202112.0139.v1.

[5] Starheim, C.C., Gomez, C., Davies, T., Lavigne, F., Wassmer, P. (2013). In-flow evolution of lahar deposits from video-imagery with implications for post-event deposit interpretation, Mount Semeru, Indonesia. *Journal of volcanology and Geothermal Research*, 256, 96-104. DOI: 10.1016/j.jvolgeores.2013.02.013.

[6] Thouret, J.C., Lavigne, F., Suwa, H., Sukatja, B., Surono. (2007). Volcanic hazards at Mount Semeru, East Java (Indonesia), with emphasis on lahars. *Bulletin of Volcanology*, 70, 221-244. DOI: 10.1007/s00445-007-0133-6.

[7] Cutler, N.A., Streeter, R.T., Dugmore, A.J., Sear, E.R. (2021). How do the grain size characteristics of a tephra deposit change over time?. *Bulletin of Volcanology*, 83(7), 45. DOI: 10.1007/s00445-021-01469-w.

[8] Darmawan, R., Juliastuti, S.R., Hendrianie, N., Rachmaniah, O., Kusnadi, N.S., Ramadhani, G.S., Tominaga, M. (2022). Effect of electrode modification on the production of electrical energy and degradation of Cr (VI) waste using tubular microbial fuel cell. *AIMS Environmental Science*, 9(4). DOI: 10.3934/environsci.2022030.

[9] Parande, A.K., Babu, B.R., Pandi, K., Karthikeyan, M.S., Palaniswamy, N. (2011). Environmental effects on concrete using Ordinary and Pozzolana Portland cement. *Construction and Building Materials*, 25(1), 288-297. DOI: 10.1016/j.conbuildmat.2010.06.027.

[10] Salamah, S.I.T.I., Wahyuni, E.T. (2018, September). The characterization of Merapi volcanic ash as adsorbent for dyes removal from batik wastewater. In *IOP Conference Series: Materials Science and Engineering* (Vol. 403, No. 1, p. 012007). IOP Publishing. DOI: 10.1088/1757-899X/403/1/012007.

[11] Yanti, F.M., Murti, S.S., Valentino, N., Pertiwi, A., Heriyanti, S.I., Sevie, G.N., IS, A.B.M. (2023). Impregnation Effect of Iron (Fe) and Cobalt (Co) on ZSM-5 Zeolite Catalyst from Rice Husk Ash and Coal Fly Ash for Methanol Synthesis. *EVERGREEN Joint Journal of Novel Carbon Resource Sciences & Green Asia Strategy*, 10 (3), 1889-1897. DOI: 10.5109/7151740

[12] Titchou, F.E., Akbour, R.A., Assabbane, A., Hamdani, M. (2020). Removal of cationic dye from aqueous solution using Moroccan pozzolana as adsorbent: isotherms, kinetic studies, and application on real textile wastewater treatment. *Groundwater for Sustainable Development*, 11, 100405. DOI: 10.1016/j.gsd.2020.100405.

[13] Di Natale, F., Lancia, A., Molino, A., Di Natale, M., Karatza, D., Musmarra, D. (2006). Capture of mercury ions by natural and industrial materials. *Journal of Hazardous Materials*, 132(2-3), 220-225. DOI: 10.1016/j.jhazmat.2005.09.046.

[14] Mu'azu, N.D., Manzar, M.S., Zubair, M., Alhajri, E.G., Essa, M.H., Meili, L., Khan, A.H. (2022). Volcanic ashe and its NaOH modified adsorbent for superb cationic dye uptake from water: Statistical evaluation, optimization, and mechanistic studies. *Colloids and Surfaces A: Physicochemical and Engineering Aspects*, 634, 127879. DOI: 10.1016/j.colsurfa.2021.127879.

[15] Silviana, S., Hasega, A.G., Hanifah, A.R.N., Sa'adah, A.N.M. (2022). Synthesis of silica coating derived from geothermal solid waste modified with 3-aminopropyl triethoxysilane (APTES) and silver nano particles (AgNPs). *EVERGREEN Joint Journal of Novel Carbon Resource Sciences & Green Asia Strategy*, 9 (4), 1224-1230. DOI: 10.5109/6625733.

[16] Gomez, C., Lavigne, F., Hadmoko, D.S., Wassmer, P. (2018). Insights into lahar deposition processes in the Curah Lengkong (Semeru Volcano, Indonesia) using photogrammetry-based geospatial analysis, near-surface geophysics and CFD modelling. *Journal of Volcanology and Geothermal Research*, 353, 102-113. DOI: 10.1016/j.jvolgeores.2018.01.021.

[17] Simatupang, L., Siburian, R., Sitanggang, P., Doloksaribu, M.E., Situmorang, M., Marpaung, H. (2018). Synthesis and application of silica gel based on mount sinabung fly ash for cd (ii) removal with fixed bed column. *Rasāyan Journal of Chemistry [RJC]*, 11(02), 819-827. DOI: 10.7324/RJC.2018.1122091.

[18] Simatupang, L. (2016). The preparation and characterization of sinabung volcanic ash silica based adsorbent. *Jurnal Pendidikan Kimia*, 8(03), 159-163. DOI: 10.24114/jpkim.v8i3.4478.

[19] Ruan, H., Nishibori, M., Uchiyama, T., Kamitani, K., Shimanoe, K. (2017). Soot Oxidation Activity of Ag / HZSM-5 (Si / Al = 40) Catalyst Soot Oxidation Activity of Ag / HZSM-5 (Si / Al = 40) Catalyst. *Evergreen Journal,* (5) 7–11. DOI: 10.5109/1928668

[20] Nabil, M., Motaweh, H.A. (2018). Porous silicon powder as an adsorbent of heavy metal (nickel). In *AIP Conference Proceedings* (Vol. 1957, No. 1). AIP Publishing. DOI: 10.1063/1.5034324.

[21] Borba, C.E., Guirardello, R., Silva, E.A., Veit, M.T., Tavares, C.R.G. (2006). Removal of nickel (II) ions from aqueous solution by biosorption in a fixed bed column: experimental and theoretical breakthrough curves. *Biochemical Engineering Journal*, 30(2), 184-191. DOI: 10.1016/j.bej.2006.04.001.

[22] Fu, F., Wang, Q. (2011). Removal of heavy metal ions from wastewaters: a review. *Journal of Environmental Management*, 92(3), 407-418. DOI: 10.1016/j.jenvman.2010.11.011.

[23] Ifijen, I.H., Itua, A.B., Maliki, M., Ize-Iyamu, C.O., Omorogbe, S.O., Aigbodion, A.I., Ikhuoria, E.U. (2020). The removal of nickel and lead ions from aqueous solutions using green synthesized silica microparticles. *Heliyon*, 6(9). DOI: 10.1016/j.heliyon.2020.e04907.

[24] Amran, F., Zaini, M.A.A. (2021). Sodium hydroxide-activated Casuarina empty fruit: Isotherm, kinetics and thermodynamics of methylene blue and congo red adsorption. *Environmental Technology & Innovation*, 23, 101727. DOI: 10.1016/j.eti.2021.101727.

[25] El Felss, N., Gharzouni, A., Colas, M., Cornette, J., Sobrados, I., Rossignol, S. (2020). Structural study of the effect of mineral additives on the transparency, stability, and aging of silicate gels. *Journal of Sol-Gel Science and Technology*, 96, 265-275. DOI: 10.1007/s10971-020-05385-x.

[26] Tome, S., Hermann, D.T., Shikuku, V.O., Otieno, S. (2021). Synthesis, characterization and application of acid and alkaline activated volcanic ash-based geopolymers for adsorptive remotion of cationic and anionic dyes from water. *Ceramics International*, 47(15), 20965-20973. DOI: 10.1016/j.ceramint.2021.04.097.

[27] Antovska, P., Cvetkovska, M., Goračinova, K. (2006). Preparation and characterization of sol-gel processed spray dried silica xerogel microparticles as carriers of heparin sodium. *Macedonian Journal of Chemistry and Chemical Engineering*, 25(2), 121-126. DOI: 10.20450/mjcce.2006.295

[28] Brinker, C.J., Scherer, G.W. (2013). Sol-gel science: the physics and chemistry of sol-gel processing, Elsevier Inc., ISBN: 9780080571034.

[29] Setyoningrum, T.M., Nandari, W.W., Murni, S.W., Nur, M.M.A. (2021). Effect of particle sizes and sodium hydroxide concentrations on silica extraction from minerals obtained in Kalirejo village, Kokap, Kulonprogo, Yogyakarta. *Eksergi*, 18(1), 29-31. DOI: 10.31315/e.v0i0.4576.

[30] Zuwanna, I., Riza, M., Aprilia, S. (2021). The impact of solvent concentration on the characteristic of silica from rice husk ash using sol gel method. In *IOP Conference Series: Materials Science and Engineering* (Vol. 1087, No. 1, p. 012060). IOP Publishing. DOI: 10.1088/1757-899x/1087/1/012060.

[31] Ma, M., Gao, K., Ma, Z., Ding, J. (2021). Influence of preparation method on the adsorptive performance of silica sulfuric acid for the removal of gaseous o-xylene. *Separation and Purification Technology*, 265, 118484. DOI: 10.1016/j.seppur.2021.118484.

[32] Naderi, M. (2015). Surface area: brunauer–emmett–teller (BET). In *Progress in filtration and separation* (pp. 585-608). DOI: 10.1016/B978-0-12-384746-1.00014-8.

[33] Omri, A., Wali, A., Benzina, M. (2016). Adsorption of bentazon on activated carbon prepared from Lawsonia inermis wood: Equilibrium, kinetic and thermodynamic studies. *Arabian journal of chemistry*, 9, S1729-S1739. DOI: 10.1016/j.arabjc.2012.04.047.

[34] Horwell, C.J., Fenoglio, I., Fubini, B. (2007). Iron-induced hydroxyl radical generation from basaltic volcanic ash. *Earth and Planetary Science Letters*, 261(3-4), 662-669. DOI: 10.1016/j.epsl.2007.07.032.

[35] Khan, K., Amin, M.N., Saleem, M.U., Qureshi, H.J., Al-Faiad, M.A., Qadir, M.G. (2019). Effect of fineness of basaltic volcanic ash on pozzolanic reactivity, ASR expansion and drying shrinkage of blended cement mortars. *Materials*, 12(16), 2603. DOI: 10.3390/ma12162603.

[36] Bariyah, S., Simatupang, L. (2021). Activation Of Sinabung Mount Volcanic Ash Using Various Mineral Acids. *Indonesian Journal of Chemical Science and Technology*, 4(1), 1-4. DOI: 10.24114/ijcst.v4i1.23087

[37] Worathanakul, P., Payubnop, W., Muangpet, A. (2009). Characterization for post-treatment effect of bagasse ash for silica extraction. *International Journal of Chemical and Molecular Engineering*, 3(8), 398-400. DOI: 10.96f0aaaabc1a19e7ae6ae3a2a975bf96705315c2

[38] Nur'aeni, D., Hadisantoso, E.P., Suhendar, D. (2017). Adsorpsi Ion Logam Mn2+ dan Cu2+ Oleh Silika Gel dari Abu Ampas Tebu. *al Kimiya: Jurnal Ilmu Kimia dan Terapan*, 4(2), 70-80. DOI: 10.15575/ak.v4i2.5087.

[39] Huriawati, F., Yuhanna, W.L., Mayasari, T. (2016). Pengaruh metode pengeringan terhadap kualitas serbuk seresah Enhalus acoroides dari Pantai Tawang Pacitan. *Bioeksperimen: Jurnal Penelitian Biologi*, 2(1), 35-43. DOI: 10.23917/bioeksperimen.v2i1.1579.

[40] Maulana Yusuf, M. (2014). Studi Karakteristik Silika Gel Hasil Sintesis dari Abu Ampas Tebu dengan Variasi Konsentrasi Asam Klorida *Doctoral Dissertation*, UIN Sunan Gunung Djati Bandung.

[41] Mori, H. (2003). Extraction of silicon dioxide from waste colored glasses by alkali fusion using potassium hydroxide. *Journal of materials science*, 38, 3461-3468. DOI: 10.1023/A:1025100901693.

[42] Setyoningrum, T.M., Murni, S.W., Nandari, W.W., Nur, M.M.A. (2021). Effect of sodium hydroxide concentrations and particle sizes on silica extraction from mineral rock obtained in Kalirejo village, Kokap, Kulonprogo, Yogyakarta. *Eksergi*, 18(1), 29-31. DOI: 10.31315/e.v0i0.4576

[43] Dhaneswara, D., Fatriansyah, J.F., Situmorang, F.W., Haqoh, A.N. (2020). Synthesis of amorphous silica from rice husk ash: comparing HCl and CH3COOH acidification methods and various alkaline concentrations. *Synthesis*, 11(1), 200-208. DOI: 10.14716/ijtech.v11i1.3335.

[44] Launer, P.J. (2013). Infrared analysis of organosilicon compounds: spectra-structure correlations. *Silicone Compd. Regist. Rev.* 175–178. DOI: 333000959

[45] Socrates, G. (2004). *Infrared and Raman characteristic group frequencies: tables and charts*. John Wiley & Sons.

[46] Azmiyawati, C., Niami, S S., Darmawan, A. (2019). Synthesis of silica gel from glass waste for adsorption of Mg2+, Cu2+, and Ag+ metal ions. In *IOP Conference Series: Materials Science and Engineering* (Vol. 509, No. 1, p. 012028). IOP Publishing. DOI: 10.1088/1757-899X/509/1/012028.

[47] Mane, P.V., Rego, R.M., Yap, P.L., Losic, D., Kurkuri, M.D. (2024). Unveiling cutting-edge advances in high surface area porous materials for the efficient removal of toxic metal ions from water. *Progress in Materials Science*, 101314. DOI: 10.1016/j.pmatsci.2024.101314

[48] Budnyak, T. M., Pylypchuk, I.V., Tertykh, V.A., Yanovska, E.S., Kolodynska, D. (2015). Synthesis and adsorption properties of chitosan-silica nanocomposite prepared by sol-gel method. *Nanoscale Research Letters*, 10, 1-10. DOI: 10.1186/s11671-014-0722-1.

[49] Sdiri, A., Higashi, T., Bouaziz, S., Benzina, M. (2014). Synthesis and characterization of silica gel from siliceous sands of southern Tunisia. *Arabian Journal of Chemistry*, 7(4), 486-493. DOI: 10.1016/j.arabjc.2010.11.007.

[50] Xu, H., Xu, D.C., Wang, Y. (2017). Natural indices for the chemical hardness/softness of metal cations and ligands. *ACS Omega*, 2(10), 7185-7193. DOI: 10.1021/acsomega.7b01039.

[51] Kuśmierek, K., Świątkowski, A. (2015). The influence of different agitation techniques on the adsorption kinetics of 4-chlorophenol on granular activated carbon. *Reaction Kinetics, Mechanisms and Catalysis*, 116, 261-271. DOI: 10.1007/s11144-015-0889-1.

[52] Ahsan, N., Shafique, U., Jamil, N., Munawar, M. A., Anwar, J. (2011). Removal of toxic dichlorophenol from water by sorption with chemically activated carbon of almond shells–A green approach. *Journal of the Chemical Society of Pakistan*, 33(6), 640.

[53] Wulandari, E., Hidayat, A.E., Moersidik, S.S. (2020). Comparison of copper adsorption effectivity in acid mine drainage using natural zeolite and synthesized zeolite. In *IOP Conference Series: Earth and Environmental Science* (Vol. 473, No. 1, p. 012143). DOI: 10.1088/1755-1315/473/1/012143.

[54] Asselah, A., Tazerouti, A. (2014). Photosulfochlorination synthesis and physicochemical properties of methyl ester sulfonates derived from lauric and myristic acids. *Journal of Surfactants and Detergents*, 17(6), 1151-1160. DOI: 10.1007/s11743-014-1635-9.

[55] Balasubramanian, C., Joseph, B., Gupta, P., Saini, N.L., Mukherjee, S., Di Gioacchino, D., Marcelli, A. (2014). X-ray absorption spectroscopy characterization of iron-oxide nanoparticles synthesized by high temperature plasma processing. *Journal of Electron Spectroscopy and Related Phenomena*, 196, 125-129. DOI: 10.1016/j.elspec.2014.02.011

[56] Holder, C.F., Schaak, R.E. (2019). Tutorial on powder X-ray diffraction for characterizing nanoscale materials. *ACS Nano*, 13(7), 7359-7365. DOI: 10.1021/acsnano.9b05157.

[57] Muktadir, G., Amro, M.D., Kummer, N., Freese, C., Abid, K. (2021). Application of x-ray diffraction (Xrd) and rock–eval analysis for the evaluation of middle eastern petroleum source rock. *Energies*, 14(20), 6672. DOI: 10.3390/en14206672